

# Corrosion behavior of a low modulus $\beta$ -Ti-45%Nb alloy for use in medical implants

R. GODLEY, D. STAROSVETSKY\*, I. GOTMAN

Faculty of Materials Engineering, Technion-IIT, Haifa 32000, Israel

E-mail: davstar@tx.technion.ac.il

The corrosion and electrochemical behavior of a low stiffness  $\beta$ -Ti-45wt.%Nb (Ti45Nb) was studied in solutions that resemble body environment, as compared to Ti6Al4V and Ti-55wt.%Ni (Ti55Ni, Nitinol) alloys currently used in surgical implants. In Ringers' solution, Ti45Nb alloy exhibited an excellent corrosion resistance, comparable to that of Ti6Al4V and much better than that of Nitinol. In acidic environments,  $\beta$ -Ti45Nb remained passive under conditions where active dissolution was observed for both Ti6Al4V and Nitinol alloys. The results warrant further corrosion and biocompatibility studies of  $\beta$ -Ti45Nb alloy to establish its suitability as implant material.

© 2006 Springer Science + Business Media, Inc.

## 1. Introduction

$\beta$ -Ti-45 wt.% Nb (Ti45Nb) alloy is a promising material for use in medical implants. An important requirement of implants designed to replace or interact with bone is a low elastic modulus matching as closely as possible that of the surrounding bone tissue [1, 2]. Bone is normally subject to stresses and strains resulting from weight bearing and movement that determine its structural organization during life. When a stiff surgical device is placed in the bone vicinity, it carries a considerable part of the load thus shielding the bone from the physiological 'stressing' required to maintain its density, strength and healthy structure. Such 'stress shielding' results in bone resorption and eventually leads to the loosening and premature failure of the implant. To prevent this undesirable phenomenon, the Young's modulus of the implant material should be as close as possible to that of the bone. Titanium and Ti6Al4V  $\alpha$ - $\beta$  alloy have the lowest elastic modulus of the currently used surgical metals ( $\sim 110$  GPa); however, their stiffness is still high compared to that of human cortical bone ( $\sim 20$  GPa). At the same time,  $\beta$ -Ti alloys, and especially those based on Ti-Nb, have significantly lower elastic moduli (Table I) and can become an attractive orthopedic material. Beta titanium alloys have been under evaluation for various implants that require moderate strength and improved ductility. BCC metastable  $\beta$ -Ti alloys possess the lowest elastic moduli among all types of Ti alloys. Some emerging clinical possibilities for the new  $\beta$ -Ti al-

loys include mandible plates, distal radius plates, spinal rods, pelvic screws, and pelvic reconstruction plates [3, 4]. Theoretical study of the effects of alloying elements on the strength and modulus of  $\beta$ -type bio-Ti alloys [5] suggests that Nb, Mo, Zr and Ta are suitable alloying elements for  $\beta$ -type Ti alloys, capable of enhancing the strength and reducing the modulus of the materials.

The properties of Ti and its alloys are being increasingly utilized in external and internal biomedical devices, e.g. orthodontic wires, cardiovascular and urological stents, bone fracture fixation plates and nails, knee and hip implants, bone substitutes, etc. [6–8]. Titanium and Ti6Al4V titanium-based alloy are the most biocompatible and corrosion-resistant implant materials currently used in surgery. For applications in the human body, surface properties and corrosion resistance are the most important material characteristics determining the biocompatibility of an implant. Implants made of Ti alloys rarely show visible signs of corrosion; nevertheless, the release of potentially harmful metal ions, such as Al and V from Ti6Al4V or Ni from Ni-Ti intermetallic, and their accumulation in the body are of great concern [9–14]. The release of nickel, whose toxicity, carcinogenicity and allergic hazards are well documented, arouses special concern. Niobium, in contrast, has never been shown or suggested as having short-term or long-term potential adverse effect [15–20].

\*Author to whom all correspondence should be addressed.

TABLE I Chemical composition and selected properties of the tested Ti-based alloys

Alloy	Ti45Nb		Ti6Al4V			Ti55Ni	
	Ti	Nb	Ti	Al	V	Ni	Ti
Composition, wt.%	55	45	90	6	4	55.6	44.4
Modulus of elasticity, GPa	62.05		105			80	
Tensile strength, MPa	550		1050			860	
Density, g/cm <sup>3</sup>	5.7		4.5			6.45	

In an earlier work [21] we have shown that, similarly to Ti6Al4V and pure titanium [22–25], a low modulus  $\beta$ -Ti45Nb alloy ( $E_{\text{Ti-Nb}} = 62$  GPa) can be made bioactive *in vitro*, i.e. can form a bone-like calcium phosphate layer on its surface. In the present work the corrosion resistance and electrochemical behavior of the alloy in Ringer's solution and in HCl solutions of different concentrations is reported. The corrosion resistance of the  $\beta$ -Ti45Nb alloy is compared to that of two Ti-based alloys currently used for surgical implants: Ti6Al4V and Ti-55 wt.% Ni (Ti55Ni, Nitinol).

## 2. Experimental

Three Ti-based alloys: low modulus  $\beta$ -Ti45Nb,  $\alpha + \beta$ -Ti6Al4V and superelastic Ti-55 wt.% Ni (Ti55Ni, Nitinol) were supplied by Performance Alloys and Materials, Ltd. Chemical composition and selected properties of the alloys are shown in Table I. The representative microstructure of the tested  $\beta$ -Ti45Nb alloy is shown in Fig. 1.

The corrosion behavior of the three Ti alloys was tested in Ringer's solution (9.00g/l NaCl, 0.4 g/l KCl, 0.20 g/l NaHCO<sub>3</sub>, 0.167 g/l CaCl<sub>2</sub>·2H<sub>2</sub>O) and in HCl solutions of different concentrations: 1M, 4M and 8M.

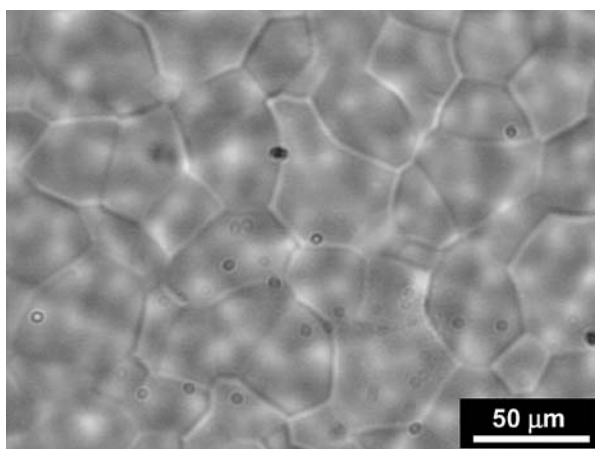


Figure 1 Representative microstructure of  $\beta$ -Ti45Nb alloy, optical microscope.

The acid solution tests were conducted in order to estimate the possibility of using Ti45Nb in low pH body locations, e.g. gastric system. The test solutions were prepared from deionized water and analytical grade reagents.

Electrochemical measurements were conducted with pencil-type electrodes. Pencil-type electrodes were made of tested alloys by mounting the 0.7 cm diameter cylinder in an epoxy resin. The cross section of the electrode was freshly wet-abraded to a 600 grit finish prior to each experiment. The experiments were performed with a potentiostat M273 EG & G. Potentials were measured using Luggin capillary.

Measurements in Ringer's solution were conducted under nitrogen atmosphere in a 0.5-l well-capped three electrodes electrochemical cell (working electrode, platinum wire as counter electrode, saturated calomel electrode (SCE) as reference electrode, nitrogen inlet and nitrogen outlet). Electrodes and gas bubblers were tightly inserted into the cell through grinded glass joints sealed with a silicone rubber sealant. Prior to testing, the medium was purged for 1 h with pure nitrogen gas in the electrochemical cell. Subsequently, the working electrode that had been positioned in the cell headspace during deaeration was immersed. The solution with the immersed sample was purged for 2 h, after which the experiment was started.

Potentiodynamic experiments in HCl solutions were conducted in the electrochemical cell without deaeration. To better interpret the test results, the three alloys (4 coupons of each alloy with a total surface area of  $\sim 10$  cm<sup>2</sup>) were immersed into the 4 M HCl solution at 37 °C and their weight loss measured after 2 h exposure. The specimens were thoroughly washed before weighed to remove any solid corrosion products that could be present on the surface.

## 3. Results and discussion

### 3.1. Ringer's solution

Fig. 2 shows polarization curves of  $\beta$ -Ti45Nb, Ti6Al4V and Ti55Ni alloys in deaerated Ringer's solution. The potential sweep (1 mV/s) was applied upon 2-h exposure at OCP. Corrosion potentials ( $E_{\text{corr}}$ ) reached at this point by the three tested alloys are given in Table II. The onset of anodic current for  $\beta$ -Ti45Nb and Ti6Al4V electrodes occurred at  $-0.63$  and  $-0.45$  V, respectively

TABLE II Corrosion potentials of tested Ti alloys measured at open circuit after 2-h exposure in deaerated Ringer's solution

Alloy	$E_{\text{corr}}$ , V
Ti45Nb	-0.646
Ti6Al4V	-0.480
Ti55Ni	-0.418

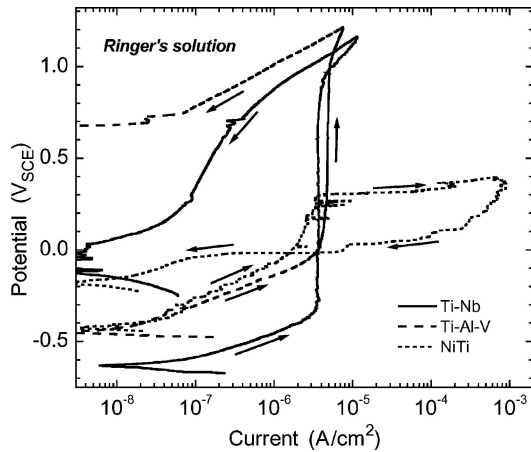


Figure 2 Potentiodynamic curves (at 1 mV/s) of  $\beta$ -Ti45Nb, Ti6Al4V and Ti55Ni alloys measured in deaerated Ringer's solution.

(Fig. 2). During the positive potential sweep both alloys remained passive in the whole tested potential region up to 1.15 V. At the back scan, anodic current rapidly decreased indicating strong passivation of  $\beta$ -Ti45Nb and Ti6Al4V electrodes during positive scan. It should be noted that anodic current measured in the region of passivity of the  $\beta$ -Ti45Nb electrode was slightly lower than that related to the passive region of Ti6Al4V. This can be attributed to the stronger passivity of  $\beta$ -Ti45Nb in the tested solution compared to Ti6Al4V.

Unlike  $\beta$ -Ti45Nb and Ti6Al4V, the Ti55Ni electrode remained passive during the positive potential sweep only in a limited potential region up to 0.28 V where breakdown occurred (Fig. 2). At further positive potential sweep the anodic current rapidly increased. The marked hysteresis between the positive and back scan parts of the anodic curve can be attributed to the onset of pitting. The numerous spikes of anodic current observed in the part of passivity region close to the breakdown are associated with metastable pit formation. Stable pits initiated by the positive potential scan at potentials above 0.28 V were repassivated at  $-0.05$  V by the back scan shift of the applied potential.

Comparing the three potentiodynamic curves in Fig. 3 one can see that the corrosion resistance of  $\beta$ -Ti45Nb alloy in Ringer's solution is better than that of Ti55Ni and is at least as good as that of Ti6Al4V, which is an accepted biocompatible surgical alloy.

## 3.2. Acid solutions

### 3.2.1. 1 M HCl solution

Potentiodynamic curves and corrosion potential transients of the three tested alloys measured in 1M HCl are shown in Fig. 3. The corrosion potential transients (Fig. 3, inset) suggest that all the three metals remain passive in 1 M HCl. For Ti55Ni and Ti6Al4V, the potentials increased after immersion reaching the values

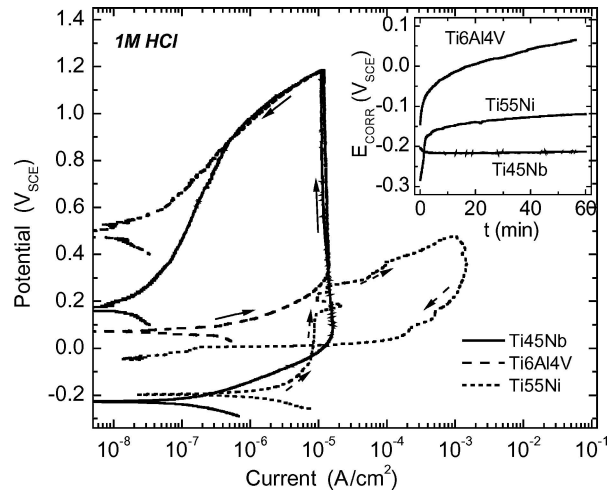


Figure 3 Potentiodynamic curves (at 1 mV/s) and corrosion potential transients (inset) of  $\beta$ -Ti45Nb, Ti6Al4V and Ti55Ni alloys measured in 1 M HCl solution.

of  $-0.12$  and  $0.07$  V, respectively, after a 1-h expose. For  $\beta$ -Ti45Nb,  $E_{\text{corr}}$  remained practically unchanged at around  $-0.22$  V.

The onset of anodic current for  $\beta$ -Ti45Nb, Ti55Ni and Ti6Al4V alloys occurred at  $-0.22$ ,  $-0.18$  and  $0.08$  V, respectively (Fig. 3). During the positive potential sweep, the electrodes made of  $\beta$ -Ti45Nb and Ti6Al4V remained passive in the whole tested potential region. Comparable values of anodic current were measured in region of passivity for both alloys. In contrast to this, Ti55Ni was only passive below 0.2 V. The rapid current increase along with the potential shift from 0.2 V to more positive values and the marked hysteresis between the positive and the backscan anodic curves are indicative of localized corrosion attack.

### 3.2.2. 4 M HCl solution

Potentiodynamic curves of the three tested alloys measured after 1-h exposure in 4M HCl are shown in Fig. 4 together with the corresponding corrosion potential transients (inset). It can be seen that  $E_{\text{corr}}$  of Ti6Al4V and Ti55Ni markedly decreased upon immersion reaching the values of  $-0.57$  and  $-0.46$  V, respectively, after a 1-h exposure. The decrease of  $E_{\text{corr}}$  indicates active dissolution of Ti6Al4V and Ti55Ni in 4M HCl. In contrast to this,  $E_{\text{corr}}$  of  $\beta$ -Ti45Nb electrode increased after 1-h expose in 4 M HCl from  $-0.3$  (upon immersion) to  $-0.2$  V indicating the alloy passivity.

The potentiodynamic curve of Ti55Ni in 4M HCl indicates active alloy dissolution with high values of anodic current. The peak of active dissolution was also detected in the anodic curve of Ti6Al4V. At  $-0.53$  V, the Ti6Al4V electrode started to undergo passivation and full passivation was achieved at  $-0.2$  V (Flade

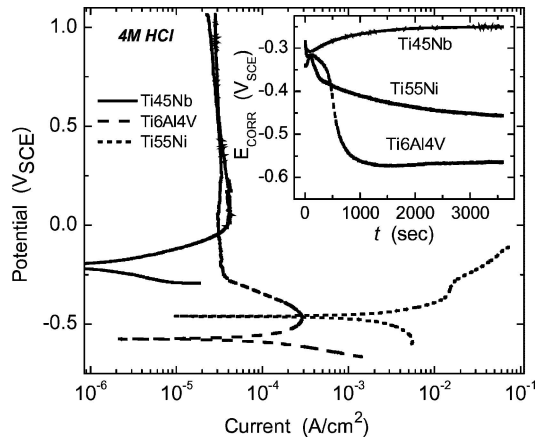


Figure 4 Potentiodynamic curves (at 1 mV/s) and corrosion potential transients (inset) of  $\beta$ -Ti45Nb, Ti6Al4V and Ti55Ni alloys measured in 4 M HCl solution.

potential). Again, the  $\beta$ -Ti45Nb electrode remained passive in the whole tested potential region.

The differences in the corrosion behavior of the three tested Ti alloys in 4 M HCl are highlighted by the results of the 2-h immersion test, Table III and Fig. 5. Weight loss measurements, Table III, produced measurable corrosion rates of 0.25 and 0.2 g/m<sup>2</sup>·h for Ti55Ni and Ti6Al4V alloy, respectively, confirming active dissolution of these two metals in 4M HCl. SEM examination of the specimens' surface after immersion revealed

TABLE III Corrosion rate of tested titanium alloys in 4 M HCl at 37 °C

Solution	Corrosion rate, g/m <sup>2</sup> ·h		
	Ti6Al4V	Ti55Ni	Ti45Nb
4 M HCl	0.200	0.254	–

distinct signs of corrosion attack on both Ti6Al4V and Ti55Ni surfaces, Fig. 5(a) and (b). In contrast to this, no measurable weight loss (Table III) and no detectable signs of corrosion (Fig. 5(d)) occurred for Ti45Nb alloy after 2 h exposure in 4 M HCl suggesting the alloy passivity under the test conditions. It is worth noting that the surface of Ti-45Nb alloy as observed in SEM remained practically unchanged even after two weeks immersion in 4 HCl.

### 3.2.3. 8 M HCl solution

As can be seen in the inset of Fig. 6,  $E_{corr}$  of  $\beta$ -Ti45Nb alloy in 8 M HCl decreased from  $-0.36$  to  $-0.44$  V after 1-h exposure indicating surface activation. In addition, a small peak of active dissolution was recorded in the potentiodynamic curve of  $\beta$ -Ti45Nb in 8 M HCl solution (Fig. 6).

### Summary

The corrosion behavior of a low modulus  $\beta$ -Ti45Nb alloy was studied potentiodynamically in neutral and

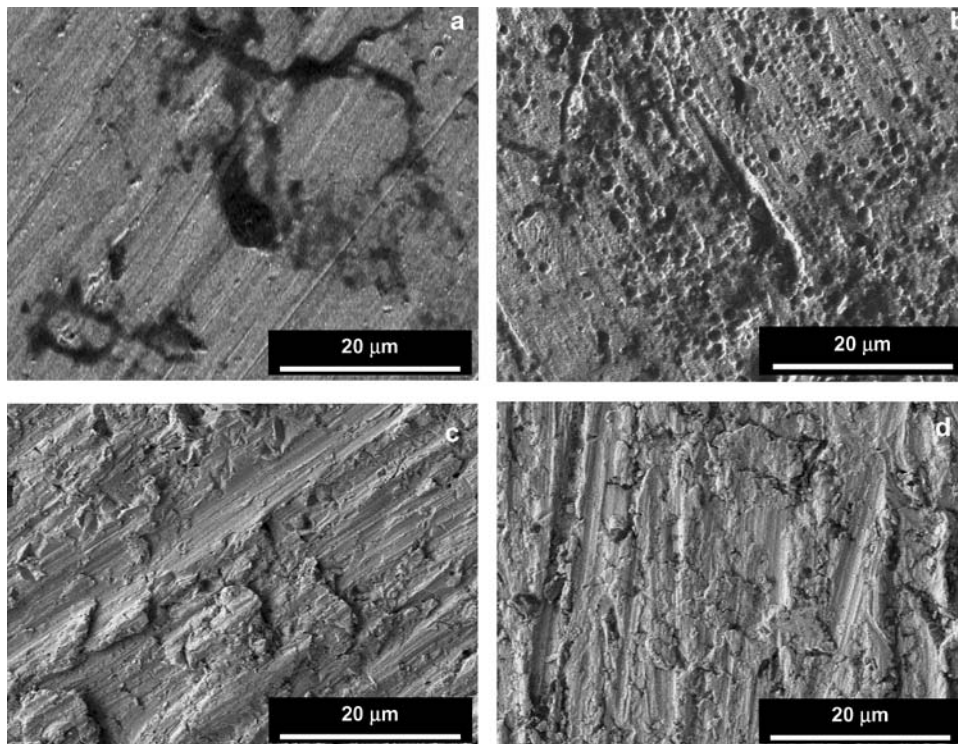


Figure 5 SEM micrographs taken from the surface of Ti6Al4V (a), Ti55Ni (b) and Ti45Nb (d) alloy coupons after 2-h immersion in 4 M HCl; c - Ti45Nb surface before immersion.

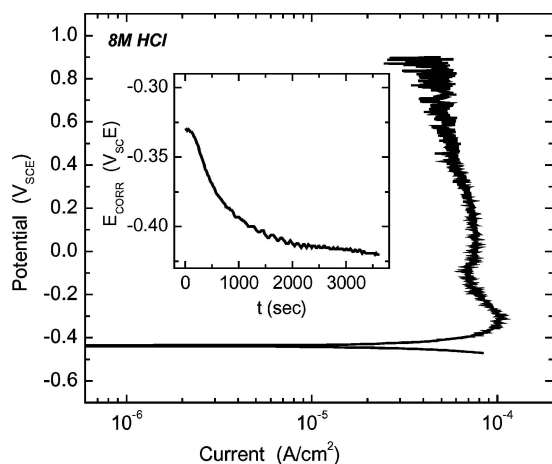


Figure 6 Potentiodynamic curve (at 1 mV/s) and corrosion potential transient (inset) of  $\beta$ -Ti45Nb alloy measured in 8 M HCl solution.

acid solutions resembling different body environments, and compared to that of Ti6Al4V and Ti55Ni alloys, both common implant metals. It has been found that in a neutral (Ringer's) solution, the Ti45Nb alloy is more corrosion resistant than Ti55Ni and at least as passive as Ti6Al4V. Potentiodynamic and weight loss tests revealed that Ti45Nb also remained passive in 4 M HCl solution for at least 2 h-conditions under which the two other Ti-based alloys underwent active dissolution. Coupled with the absence of reported toxicity for Nb, the results of the present work suggest that  $\beta$ -Ti45Nb alloy could be more biocompatible than Ti6Al4V. Further studies are required to establish the extent of Ti45Nb biocompatibility and its suitability as implant material.

### Acknowledgement

This work was supported by the German-Israeli Foundation for Scientific Research and Development (GIF) through research grant No. I-810-236.10/2003.

### References

1. D. A. PUELO and A. NANCY *Biomaterials* **20** (1999) 2311.
2. F. PIPINO, *J. Orthop. Traum.* **1** (2000) 3.
3. J. A. DISEGI, *Int. J. Care Injured* **31** (2000) S-D14.
4. E. D. JOSEPH and D. BRONZINO, *The Biomedical Engineering Handbook*, 2nd Ed. CRC Press UC 2000.
5. Y. SONG, D.S. XU, R. YANG, D. LI, W. T. WU and Z. X. GUO, *Mater. Sci. Eng. R* **36** (2002) 143.
6. D. H. KOHN, *Current Opinion Solid State Mater. Sci.* **3** (1998) 309.
7. L. L. HENCH, *Current Orthop.* **14** (2000) 7.
8. L. L. HENCH and J. M. POLAK, *Science* **295** (2002) 1014.
9. A. REMES and D. F. WILLIAMS, *Biomaterials* **13** (1992) 731.
10. L. S. CASTELMAN and S. M. MOTZKIN, in: *Biocompatibility of clinical implant materials*, edited by D. F. Williams. Boca Raton, FL., CRC Press (1981) p. 129.
11. BLACK J., *Biological performance of materials, Fundamentals of biocompatibility*. NewYork: Dekker, 1992.
12. D. STAROSVETSKY, A. SHENHAR and I. GOTMAN, *J. Mater. Sci.: Mater. Med.* **12** (2001) 145.
13. D. STAROSVETSKY, O. KHASELEV and J. YAHALOM, *Corrosion* **54** (1998) 525.
14. D. STAROSVETSKY and I. GOTMAN, *Biomaterials* **22** (2001)1853.
15. E. EISENBARTH. D. VELTEN, M. MÜLLER, R. THULL and J. BREME, *Biomaterials* **25** (2004) 5705.
16. T. HANAWA, *Mater. Sci. Eng. C* **24** (2004) 745.
17. M. KHAN, R. WILLIAMS and D. WILLIAMS, *Biomaterials* **20** (1999) 631.
18. M. SEMLITSCH, H. WEBER, R. STREICHER and R. SCHON, *ibid.* **13** (1992) 781.
19. C. PYPEN, K. DESSEIN, J.A. HELSEN, M. GOMES, H. LEENDERS and J.D. DE BRUIJN, *J. Mater. Sci.: Mater. Med.* **9** (1998) 761.
20. MITSUO NIINOMI, *Biomaterials* **24** (2003) 2673.
21. R. ROSENBERG, D. STAROSVETSKY and I. GOTMAN, *J. Mater. Sci. Lett.* **22** (2003) 29.
22. S. NISHGERU, H. KATO, H. FUJITA, M. OKA, H.M. KIM. T. KOKUBO and T. NAKAMURA, *Biomaterials* **22** (2001) 2525.
23. L.L. HENCH, *J. Biomed. Mater. Res.* **41** (1998) 511.
24. H.B. WEN, J.G.C. WOLKE, J.R. WIJN, Q. LIU and F.Z. CUI, *Biomaterials* **18** (1997) 1471.
25. S. NISHIGUCHI, T. NAKAMURA, M. KOBAYASHI, H.M. KIM, F. MIYAJI and T. KOKUBO, *ibid.* **20** (1999) 491.

Received 5 May 2004  
and accepted 25 May 2005